International Journal of Research in Engineering and Science (IJRES)
ISSN (Online): 2320-9364, ISSN (Print): 2320-9356
www.ijres.org Volume 10 Issue 10 ǁ October 2022 ǁ PP. 470-474

Effect of Confining Pressure on the Stress Paths of Soils Using MIT and Cambridge Plots Methods

Idoniboyeobu, L. O., Akpila, S.B.& Jaja, G. W. T.
Department of Civil Engineering, Rivers State University Port Harcourt,
P.M.B. 5080, Port Harcourt, Nigeria.

ABSTRACT
The effect of confining pressure on the stress paths of soils was carried out on 20 soil samples which were obtained from two locations: Obuama Community in Degema Local Government Area and Rivers State University in Port Harcourt Local Government Area of Rivers State. The soil samples were examined through laboratory tests and results of AASHTO classification system revealed the soils are generally A-4 to A-7-5. Results from unconsolidated undrained triaxial tests on confining cell pressures of 50 kN/m², 100 kN/m², 150 kN/m², 200 kN/m², 250 kN/m² and 300 kN/m² respectively gave constant angle of the failure plane to the major principal plane, the MIT system gave 47.8^0 while the Cambridge system gave 59.2^0. Consequently, increase in cell pressure does not have an effect on each of the stress path of the soil as the angle of failure plane to the major principal plane, remains the same.

Date of Submission: 08-10-2022 Date of acceptance: 18-10-2022

I. INTRODUCTION

The deviatoric failure loads of soils are influenced by the confining cell pressures applied to them. Confining pressure is the stress or pressure forced on a layer of soil or rock by the heaviness of the overlying substance, which alters the behavior of the materials. (Alkire & Andersland, 2017). When confining pressure is applied to a soil mass, it usually causes a strain in the soil, resulting in the stress-strain relationship.

Confining cell pressures of 100 kN/m², 200 kN/m² and 300 kN/m² are commonly used in the laboratory in determining shear strength parameters. However, BS 1377: Part 7: 1990 recommends that for undisturbed normally-consolidated soil, cell pressures of $0.5\sigma_v$, σ_v and $2\sigma_v$ might be appropriate; where σ_v is the total vertical in-situ stress. For shallow foundations, these recommended cell pressures appear unrealistic as they seem too insignificant to generate the necessary pressure during the consolidation phase in the triaxial test.

Cohesive soil is common in the field of geotechnical engineering. It is a fine-grained soil of low-strength, exhibits plasticity and is easily deformable due to its high percentage of silt and clay materials (Kimiaghalam*et al*., 2016). Generally, soils undergo stresses due to the load or pressures exerted on them (Akpila & Omunguye, 2014). These stresses may lead to failure, depending on the shear strength of the soil. The response observed from the soil when these pressures are applied, are usually used in the design of geotechnical structures (Joseph, 2012).

The test performed to determine the behavior of the soil under confined cell pressure is the Triaxial Compression Test (Fig 1.1). Confining pressures are usually exerted into the triaxial cell in form of water during the consolidation phase. This confining pressure is also known as the minor principal stress and is kept in the cell throughout the test and when drainage is not permitted, it is called a total stress test. In the shearing phase, the deviator stress is applied incrementally to the soil causing shearing and thus, helps to determine the shear strength of the soil (Rees,2013).

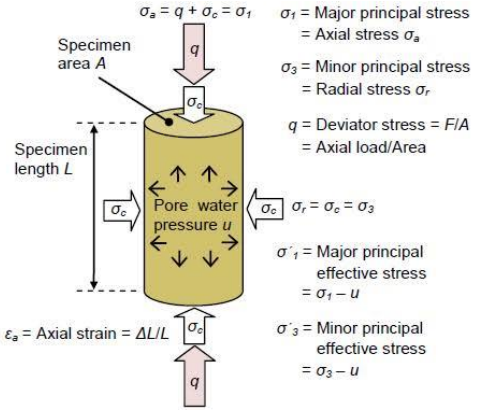

Figure 1.1: UU Triaxial Compression Test Process Diagram
Source: (Rees, 2013)

Various geotechnical engineering structures are governed by the disturbance during loading and unloading of stresses (Wang*et al*, 2018). Since the soil exhibits different responses during the loading and unloading processes, the confining pressure, which can affect the behavior of the soil, is an important factor to consider when determining the shear strength of the soil (Wang*et al*, 2018).

The stresses that occur in the soil sample during loading and unloading are usually monitored and plotted in the Mohr-coulomb diagram as Mohr circles (Baral,2020). However, it can be difficult and confusing to plot a large number of circles in the Mohr-Coulomb diagram. Therefore, for easy presentation, this consecutive state of the stresses is represented by a set of stress points in a pathway known as the stress path (Ubani, 2021).

A stress path is therefore, a pathway that shows the sequential states of stress that occur in a soil specimen during loading and unloading. Two techniques were used for the graphical representation of the stress path and they are:

i. Cambridge Plot

For three dimensional stresses, the stress path is plotted based on the Mohr circle failure envelope and is known as the Cambridge stress path. It takes into consideration, the major principal stress (σ_1), the intermediate principal stress (σ_2) and the minor principal stress (σ_3). We can define the coordinates as represented in Equations (2.1) and (2.2) respectively.

$$p = \sigma_1 - \sigma_3 \quad (2.1)$$

$$q = \frac{1}{3}(\sigma_1 + 2\sigma_3) \quad (2.2)$$

where p and q represent the mean stress and deviator stress, respectively.

ii Massachusetts Institute of Technology (MIT) Plot

For two-dimensional stresses, the stress path is plotted based on the Mohr circle (the maximum shear stress failure envelope). This stress path is known as the MIT stress path. It takes into consideration, the major principal stress (σ_1) and the minor principal stress (σ_3) only. The intermediate principal stress is ignored, as it is assumed to be equal to the minor principal stress. Since it is a two-dimensional plot, it is suitable for a plane stress condition. We can define the coordinates as in Equations (2.3) and (2.4) respectively.

$$s = \frac{\sigma_1+\sigma_3}{2} \quad \text{or} \quad s = \frac{\sigma_v+\sigma_h}{2} \quad (2.3)$$

$$t = \frac{\sigma_1-\sigma_3}{2} \quad \text{or} \quad t = \frac{\sigma_v-\sigma_h}{2} \quad (2.4)$$

where s and t are the radius and center of the Mohr's circle, and represent the mean stress and maximum shear stress, respectively. Fig. 1.2 shows a typical stress path diagram.

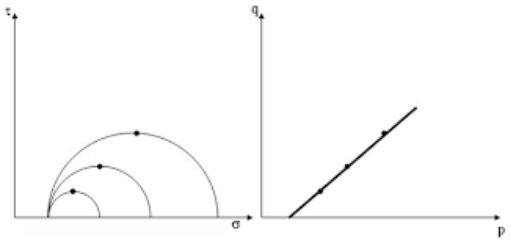

Figure 1.2: Stress Path Diagram
Source: (Ubani, 2021)

II. MATERIALS AND METHODS

2.1. Materials

2.1.1. Cohesive Soil

The soil samples collected for this research were generally A-4 to A-7-5 soils, as classified under the AASHTO classification system. The samples were collected under weather conditions of 24^0C – 31^0C.

2.1.2. Triaxial Testing Equipment and Its Accessories

The triaxial equipment is made up of:

i. The triaxial cell, which is made of heavy clear acrylic for maximum visibility and designed to minimize corrosion. It includes a loading piston whose capacity is designed to accept high axial loads during the tests. The capacity of the cell can carry confining pressures as high as 1700kPa which is enough for stimulating most in-situ conditions. It also includes accessories such as O-rings, porous stones that help fit the samples in the cell.

ii. The control panels, which allow for the control and monitoring of fluid and air pressures in the triaxial chamber.
iii. Other accessories such as the venier caliper, the spatula and latex membrane for preparing, trimming, mounting and measuring the soil samples.

2.2. Methods

The following methods were used during the research

2.2.1. Sampling of Materials

The soil samples used for this research was gotten from two locations, namely: Rivers State University in Phalga LGA and Obuama, in Asari-Toru LGA. A total of 10 samples were collected at a depth of 2m. The samples were completely sealed to avoid loss or gain of moisture. They were then taken to the laboratory for testing.

2.3. Stress Paths

The stress paths were presented in a plot to study the stress changes in the soil caused from the loading conditions during the triaxial test. The stress paths were plotted in a total stress condition using two approaches: The MIT plot and the Cambridge plot.

III. RESULTS AND DISCUSSION

3.1. Stress Path

The results of successive stresses in the soils are presented, adopting the Cambridge plot (Figure 3.1-3.2) and MIT plot (Figures 3.3-3.4).

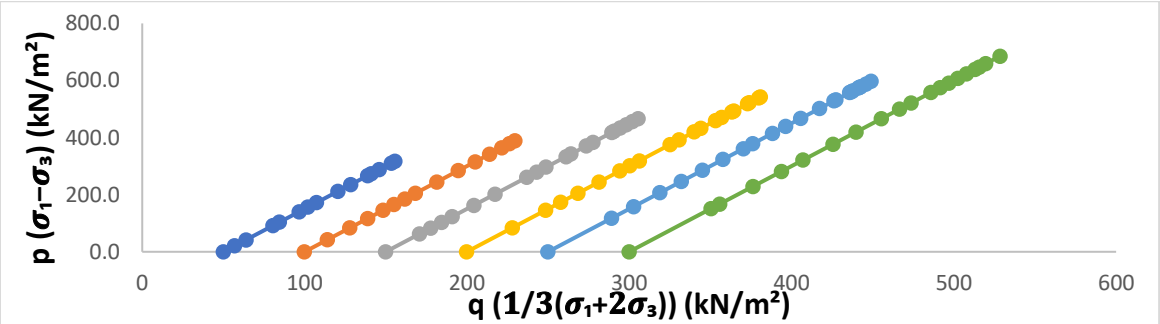

Figure 3.1: Cambridge Plot for a Typical Borehole

Figure 3.1 shows a progressive increase in the stresses from incremental loading. It also shows the angle of inclination to the major principal plane remained the same despite the increase in the confining pressure for all the soil samples. Here, the angle of inclination of the failure plane to the major principal plane is 59.2^0.

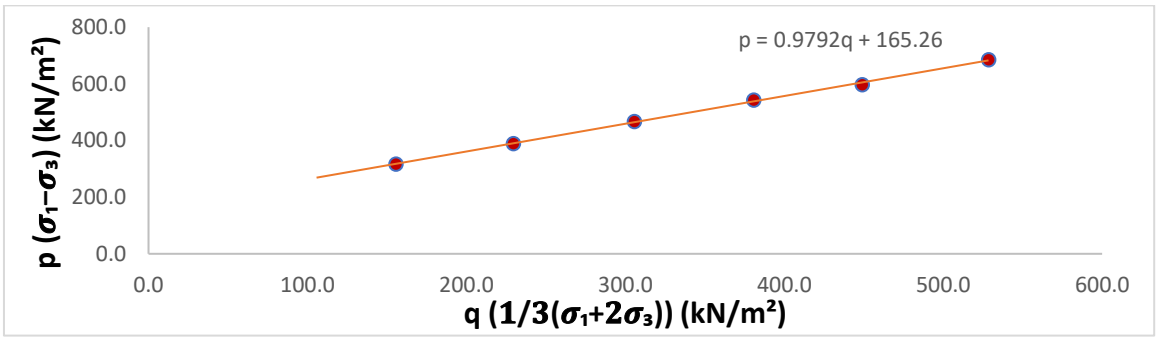

Figure 3.2: Cambridge Plot Failure Envelope for a Typical Borehole

Figure 3.2, the maximum deviatoric stress P at various cell pressures is depicted to represent the failure envelope for the soil. The model equations from the failure envelope for each of the soil samples are presented inTable 3.1.

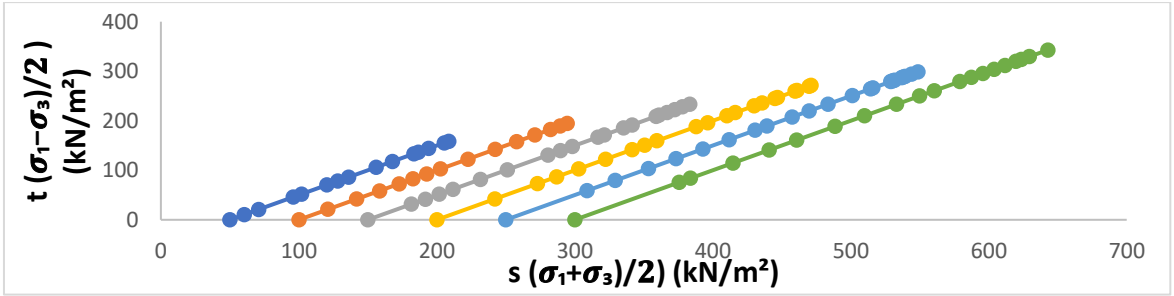

Figure 3.3: MIT Plot for a Typical Borehole

Similarly, figure 3.3 shows a progressive increase in the stresses from incremental loading. The angle of inclination of the failure plane to the major principal plane remained the same despite the increase in the confining pressure in all the soil samples. The average angle of inclination of the failure plane to the major principal plane is 47.8°.

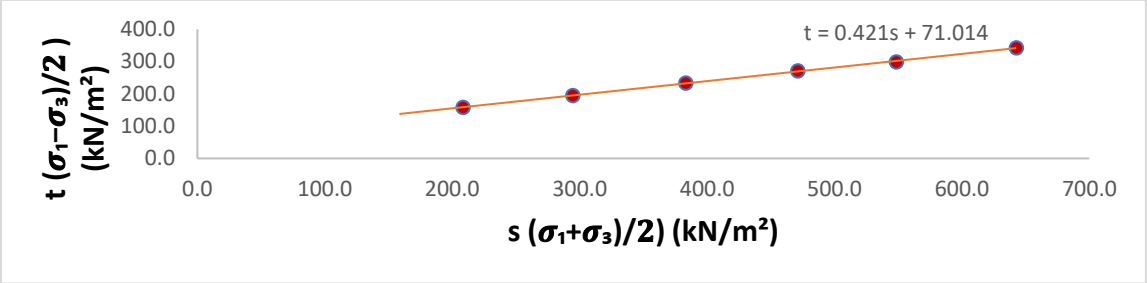

Figure 3.4: MIT Plot Failure Envelope for a Typical Borehole

In figure 3.4, the maximum deviatoric stress t at various cell pressures represents the failure envelope of the soils for the MIT method. The model equations from the failure envelope for each of the soil samples are presented in Table 3.2.

The $\theta - \emptyset$ relationship was derived from the stress path diagram are as follows:

$\theta = 27.5 + \frac{\emptyset}{2}$ (Cambridge Plot)

$\theta = 37.5 + \frac{\emptyset}{2}$ (MIT)

Table 3.1: Model Equations for Cambridge Stress Path Failure Loads

Location /Borehole No.	Rivers State University (RSU)	Location /Borehole No.	Obuama Community (DEGEMA LGA)
1	p = 246.46+0.6501q	**11**	p = 186.18+0.4835q
2	p = 260.46+0.6287q	**12**	p = 188.32+0.3603q
3	p = 165.13+0.4051q	**13**	p = 176.39+0.3935q
4	p = 200.88+0.9666q	**14**	p = 191.53+0.4409q
5	p = 118.28+0.4399q	**15**	p = 209.32+0.3437q
6	p = 216.64+0.2757q	**16**	p = 143.16+1.0531q
7	p = 256.38+0.5317q	**17**	p = 208.83+0.9533q
8	p = 134.86+0.5971q	**18**	p = 165.26+0.9792q
9	p = 186.7+0.9744q	**19**	p = 253.15+0.6445q
10	p = 265.17+ 0.6227q	**20**	p = 217.63+0.2888q

Table 3.2: Model Equations for MIT Stress Path Failure Loads

Location/ Borehole No.	Rivers State University (RSU)	Location/ Borehole No.	Obuama Community (DEGEMA LGA)
1	t = 109.85+0.2965s	11	t = 85.739+0.2249s
2	t = 116.85+0.2874s	12	t = 88.169+0.172s
3	t = 77.289+0.1899s	13	t = 82.404+0.1858s
4	t = 86.286+0.4167s	14	t = 89.095+0.2057s
5	t = 54.665+0.2064s	15	t = 98.918+0.1628s
6	t = 102.97+0.1336s	16	t = 60.741+0.4483s
7	t = 116.22+0.2482s	17	t = 89.748+0.4121s
8	t = 61.09+0.2722s	18	t = 71.014+0.421s
9	t = 80.128+0.4196s	19	t = 111.76+0.2972s
10	t = 118.79+0.2853s	20	t = 103.65+0.1383s

IV. CONCLUSION

Based on the study, the following conclusion can be drawn.

i. The soils were generally classified as inorganic clays of low to medium plasticity.

ii. Increase in confining pressure had no effect on the angle of the stress paths to the major principal plane as they remained the same through all cell pressures for each soil sample.

iii. The $\theta - \emptyset$ relationship derived from the stress path diagram are as follows:

$\theta = 27.5 + \frac{\emptyset}{2}$ for 3 dimensional stresses

$\theta = 37.5 + \frac{\emptyset}{2}$ for 2 dimensional stresses

These models can be used in evaluating the angle of inclination of the failure plane to the major principal planes

REFERENCES

[1]. Akpila, S. B. & Omunguye, I. W. (2014). Soil Modulus and Undrained Cohesion of Clayey Soils from Stress - Strain Models, *Canadian Journal of Pure and Applied Sciences*, 8(3), 3155-3161.

[2]. Akpila, S. B. & Omunguye, I. W. (2015). Derivative of stress and undrained cohesion modela based onsoil modulus of cohesive soils. *International Journal of Civil Engineering and Technology*, 6(7), 32-40.

[3]. Alkire, B., & Andersland, O. (2017). The Effect of Confining Pressure on the MechanicalProperties of Sand–Ice Materials. *Journal of Glaciology,12*(66), 469-481.

[4]. Backus, B. E. (2021). Triaxial Shear Testing of Soils, Understanding Methods and Equipment.444-456.

[5]. BS 1377: 1975 Method of tests for soils for civil engineering purposes.

[6]. Kimiaghalam, N., Clark, S. P,& Ahmari, H. (2016). An experimental study on the effects of physical, mechanical, and electrochemical properties of natural cohesive soils on critical shear stress and erosion rate. Int J Sediment Res, New Jersey 3(1), 1–15

[7]. Labuz, J.& Zang, A. (2012). Mohr-Coulomb Failure Criterion. - Rock Mechanics and Rock Engineering. Department of Civil Engineering, University of Minnesota, Minneapolis.USA. 45(6), 975-979.

[8]. Rees, S. (2013). Introduction to triaxial testing, Part one. Published on the Geotechnical Specialist at GDS website www.gdsinstruments.com. 3(1), 9-12.

[9]. Ubani O. (2021). Stress Path Approach for Shear Strength of Soils. Structureville Research Services, New York.

[10]. Wang, S., Hagan, P., Zhao, Y., Chang, K.& Zou, Z. (2018). The Effect of Confining Pressure and Water Content on Energy Evolution Characteristics of Sandstone under Stepwise Loading and Unloading. *Advances in Civil Engineering.*